NPL
National Physical Laboratory

NPL REPORT IR 68

AVERAGE DISTANCES AND ANGLES FOR RADIATION ARRIVING AT A MEASUREMENT POINT FROM A CIRCULAR SOURCE AREA

DAVID THOMAS AND KIM WARD

DECEMBER 2024

Average distances and angles for radiation arriving at a measurement point from a circular source area

David Thomas and Kim Ward
Nuclear Metrology Group, Medical Marine and Nuclear, NPL

ABSTRACT

A determination of the intensity and average angle of incidence for radiation from a surface source at a point away from the surface involves the integration of distances and angles over the area of the source. This report derives the equations for performing these calculations for a circular source. A Fortran program that can be used for performing these calculations is described, and results are presented for average distances, relative intensities, and angles for the radiation in the NPL thermal column where the source is a circular area at the bottom of a vertical column.

ISSN 1754-2952

https://doi.org/10.47120/npl.IR68

National Physical Laboratory

Hampton Road, Teddington, Middlesex, TW11 0LW

This work was funded by the UK Government's Department for Science, Innovation & Technology through the UK's National Measurement System programmes.

Approved on behalf of NPL by
Ben Russell, Science Area Leader.

CONTENTS

1. Introduction

When calibrating a radiation measuring device in the field from a source of radiation the usual approach is to position the reference point of the device at a specific point, called 'the point of test', in the radiation field [(1)]. With this approach the characteristics of the field at the point of test must be known. These include the intensity and the angular dependence of the radiation field. Ignoring the effects of scatter of the radiation in the air and the surrounding walls, floor, and ceiling of a calibration room, both the intensity and angular characteristics of the un-scattered field depend only on the distance to the source and its size. The intensity of radiation from a point source has an inverse square law dependence on the distance from the source, i.e. if the distance is l, the intensity, ignoring air attenuation, will be proportional to $1/l^2$. If l is large enough the radiation at the point of test is approximately unidirectional.

Although many sources used for calibrations approximate to a point, there are other possible configurations. This document investigates the variation of intensity and angle of incidence for radiation from a plane circular source with uniform intensity over its area for measurement points located at different distances from the source. Specifically, if l is the distance from the point of test to any point on the surface source the document presents equations for calculating, L_a, the average value of $1/l^2$ and thus a measure of the radiation fluence, for ϕ_a the average angle of incidence, and for the fluence-weighted average angle of incidence ϕ_{fwa}. It also gives equations for l_a, the average value of l, in order to compare L_a with $1/l_a^2$.

2. Points on the axis of the circle

The simplest calculations are for points on a perpendicular line through the centre of the source and the geometry for this is shown in Figure 1.

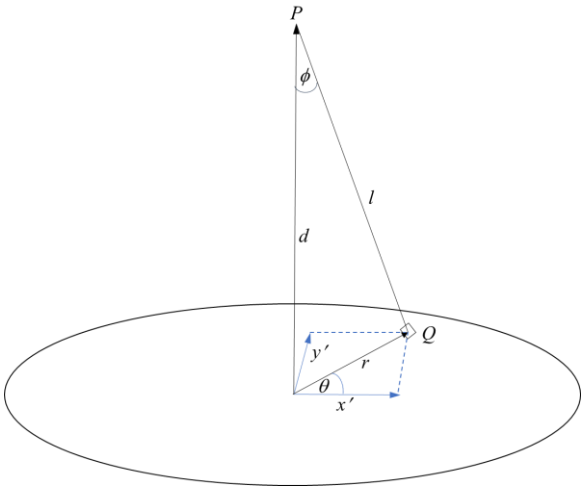

Figure 1. Distances and angles involved in calculations for points on a perpendicular line through the centre of a circular source.

Assumptions made in deriving the equations for the quantities of interest are:

a) The surface source is a circle of radius R.
b) The emission from the source is uniform over the circular area.
c) Any point within the circle can be thought of as a point source with the intensity of the radiation from that point falling off according to the inverse square law. This is the equivalent of assuming isotropic emission into 2π for any point on the circular surface.

The amount of radiation reaching point *P* from an element of the surface source at *Q* is proportional to the area at *Q*. Because the area is on a circle the equations are best expressed in spherical polar coordinates where the area element can be written as $r\,\mathrm{d}\theta\,\mathrm{d}r$. If *f* represents any of the three quantities of interest, $1/l^2$, ϕ, and *l*, then the value, f_a, when the quantity is averaged over the circle, is given by:

$$f_a = \frac{\int_0^R \int_0^{2\pi} f \cdot r\,\mathrm{d}r\,\mathrm{d}\theta}{\int_0^R \int_0^{2\pi} r \cdot \mathrm{d}r\,\mathrm{d}\theta} = \frac{\int_0^R \int_0^{2\pi} f \cdot r\,\mathrm{d}r\,\mathrm{d}\theta}{\pi R^2} \tag{1}$$

Since $l^2 = d^2 + r^2$ and $\phi = \arctan(r/d)$ the equations for the average values of the three quantities of interest are reasonably simple and can be solved analytically.

For the average L_a of the inverse square distance $1/l^2$:

$$L_a = \frac{1}{\pi R^2} \int_0^R \int_0^{2\pi} 1/(d^2 + r^2) \cdot r\,\mathrm{d}r\,\mathrm{d}\theta \tag{2}$$

The terms in the equation are independent of the azimuthal angle θ so it can be written as:

$$\begin{aligned} L_a &= \frac{2\pi}{\pi R^2} \int_0^R 1/(d^2 + r^2) \cdot r\,\mathrm{d}r = \frac{2}{R^2}\left[\frac{\ln(d^2 + r^2)}{2}\right]_0^R \\ &= \frac{1}{R^2}\left[\ln(d^2 + R^2) - \ln(d^2)\right] = \frac{1}{R^2}\ln\left(1 + \frac{R^2}{d^2}\right) \end{aligned} \tag{3}$$

The equation for the average angle ϕ_a is:

$$\phi_a = \frac{1}{\pi R^2} \int_0^R \int_0^{2\pi} \arctan(r/d) \cdot r\,\mathrm{d}r\,\mathrm{d}\theta \tag{4}$$

The terms in the equation are again independent of the angle θ so it can be solved to give:

$$\begin{aligned} \phi_a &= \frac{2\pi}{\pi R^2} \int_0^R \arctan(r/d) \cdot r\,\mathrm{d}r = \frac{2}{R^2} \cdot \frac{1}{2}\left[(r^2 + d^2)\arctan\left(\frac{r}{d}\right) - r \cdot d\right]_0^R \\ &= \frac{1}{R^2}\left[(R^2 + d^2)\arctan\left(\frac{R}{d}\right) - R \cdot d\right] = \left[\left(1 + \frac{d^2}{R^2}\right)\arctan\left(\frac{R}{d}\right) - \frac{d}{R}\right] \end{aligned} \tag{5}$$

Finally, the equation for the average distance l_a is:

$$l_a = \frac{2\pi}{\pi R^2} \int_0^R \sqrt{d^2 + r^2} \cdot r\,\mathrm{d}r = \frac{2}{R^2}\left[\frac{(r^2 + d^2)^{3/2}}{3}\right]_0^R = \frac{2}{R^2}\left(\frac{(R^2 + d^2)^{3/2}}{3} - \frac{d^3}{3}\right) \tag{6}$$

Although the above results are completely general the main reason for this work was to determine these quantities for a specific circular source.

The thermal neutron column at NPL consists of a 30 cm diameter cadmium-lined steel column that can have a length of 1 m or 1.5 m. The neutrons emerge from an area of graphite within the thermal pile below this vertical column which effectively defines a 30 cm diameter disc source [(2)]. The facility thus has the type of source, i.e. a plane circular source, with uniform intensity over its area, assumed in the derivation here of the equations for average distances and angles. Devices can be irradiated in the beam defined by the column at any distance from the source plane, although typical irradiation distances are in the range 100 to 200 cm.

The results of calculations for a circle of radius 15, corresponding to that in the column, are displayed in Table 1 for values of d from 1 to 500. Values for L_a, ϕ_a, and l_a, are presented. The units of the distances are not given as all the calculated quantities depend only on the ratios of distances. The quantities $1/d^2$ and $1/l_a^2$ are approximations to L_a as d becomes larger, and the table also lists these quantities and the percentage differences between the various estimates.

Table 1. Values for l_a, L_a and ϕ_a calculated from equations (6), (3), and (5) for a circle of radius 15 and various distances d.

d	l_a	Diff. d & l_a	$1/d^2$	$1/l_a^2$	L_a	Diff. L_a & $1/d^2$	Diff. L_a & $1/l_a^2$	ϕ_a
0	10.0	-	∞	1.00×10^{-2}	-	-	-	90.00°
1	10.1	906%	1.00	9.87×10^{-3}	2.41×10^{-2}	4051%	-59.0%	82.75°
2	10.2	412%	2.50×10^{-1}	9.53×10^{-3}	1.80×10^{-2}	1290%	-47.0%	76.23°
5	11.3	127%	4.00×10^{-2}	7.77×10^{-3}	1.02×10^{-2}	291%	-24.0%	60.42°
10	14.4	44.0%	1.00×10^{-2}	4.82×10^{-3}	5.24×10^{-3}	90.9%	-7.90%	43.14°
15	18.3	21.9%	4.44×10^{-3}	2.99×10^{-3}	3.08×10^{-3}	44.3%	-2.90%	32.70°
20	22.6	13.0%	2.50×10^{-3}	1.96×10^{-3}	1.98×10^{-3}	26.0%	-1.23%	26.02°
30	31.8	6.01%	1.11×10^{-3}	9.89×10^{-4}	9.92×10^{-4}	12.0%	-0.31%	18.23°
40	41.4	3.44%	6.25×10^{-4}	5.84×10^{-4}	5.85×10^{-4}	6.88%	-0.11%	13.94°
50	51.1	2.22%	4.00×10^{-4}	3.83×10^{-4}	3.83×10^{-4}	4.44%	-0.05%	11.26°
75	75.7	0.99%	1.78×10^{-4}	1.74×10^{-4}	1.74×10^{-4}	1.99%	-0.01%	7.58°
100	100.6	0.56%	1.00×10^{-4}	9.89×10^{-5}	9.89×10^{-5}	1.12%	0.00%	5.69 °
125	125.4	0.36%	6.40×10^{-5}	6.35×10^{-5}	6.35×10^{-5}	0.72%	0.00%	4.57°
150	150.4	0.25%	4.44×10^{-5}	4.42×10^{-5}	4.42×10^{-5}	0.50%	0.00%	3.81°
175	175.3	0.18%	3.27×10^{-5}	3.25×10^{-5}	3.25×10^{-5}	0.37%	0.00%	3.27°
200	200.3	0.14%	2.50×10^{-5}	2.49×10^{-5}	2.49×10^{-5}	0.28%	0.00%	2.86°
500	500.1	0.02%	4.00×10^{-5}	4.00×10^{-6}	4.00×10^{-6}	0.04%	0.00%	1.15°

The variation of the intensity, L_a with distance d is plotted in Figure 2 where it is compared with two approximations, $1/d^2$ and $1/l_a^2$, for this quantity. At larger values of d, $1/d^2$ is a reasonable estimate of L_a although, from the data in Table 1, the difference is still about 2% at 100 cm. The quantity $1/l_a^2$ is a better estimate of L_a, but at smaller distances these two quantities also diverge the difference being -0.05% at 50 cm increasing to -7.9% at 10 cm.

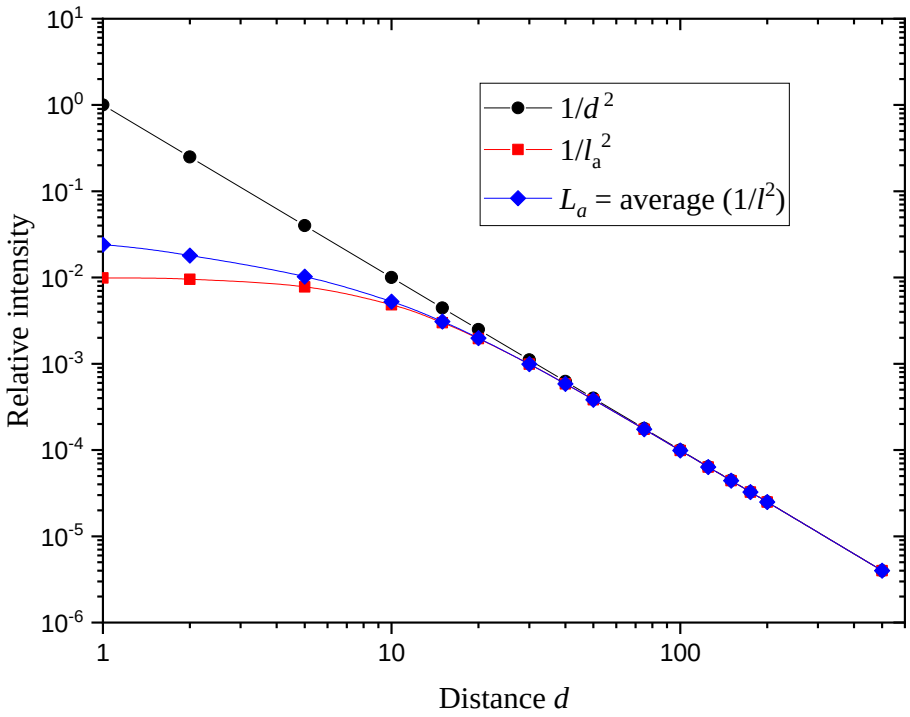

Figure 2. Variation of L_a the intensity of radiation as a function of the distance from a circular source of radius 15 and comparison with two approximate expressions.

At the larger distances the range of angles of incidence of the radiation from a circular source at a point is small, but this range increases as the distance d decreases, and the average angle of incidence thus increases.

By using eq. (5) the variation of the average angle of incidence ϕ_a subtended by points on a circle can be calculated for points at distance d from the circle along the axis through the centre of the circle. Values are presented in Table 1, however, this does not give the average angle for radiation incident at the reference point. To calculate this quantity each angle must be weighted by the fluence at that angle. As the fluence is proportional to the inverse square of the distance from the point on the source circle to the reference point, the weighting factor can be written as $1/(d^2+r^2)$, and the equation for the fluence-weighted average angle, ϕ_{fwa}, is, c.f. eq.(4):

$$\phi_{fwa} = \frac{\int_0^R \int_0^{2\pi} \arctan(r/d)/(d^2+r^2)\cdot r \,\mathrm{d}r \,\mathrm{d}\theta}{\int_0^R \int_0^{2\pi} 1/(d^2+r^2) r \cdot \mathrm{d}r \,\mathrm{d}\theta} = \frac{2}{L_a R^2}\int_0^R \arctan(r/d)/(d^2+r^2)\cdot r \,\mathrm{d}r \qquad (7)$$

Although all the terms in the equation are independent of the azimuthal angle θ, the integral does not have a simple solution, and calculation of the fluence-weighted averaged incidence angle for the radiation requires a numerical integration approach. This is covered in the next section for the more general case of a reference point anywhere in a plane above the circular source, not just for points on a normal from the centre of the source.

3. Points in a plane above the circle

One type of irradiation regularly performed in the thermal column neutron beam at NPL is of personal dosemeters on a phantom. This phantom may be tilted to provide calibrations for angles of incidence other than zero degrees. This means there is a need to know the intensity and average angle of incidence at points other than those on a perpendicular line through the centre of the circle. The face of the phantom onto which the dosemeters are attached is a square and the distances and angles for a point on a square are shown in Figure 3.

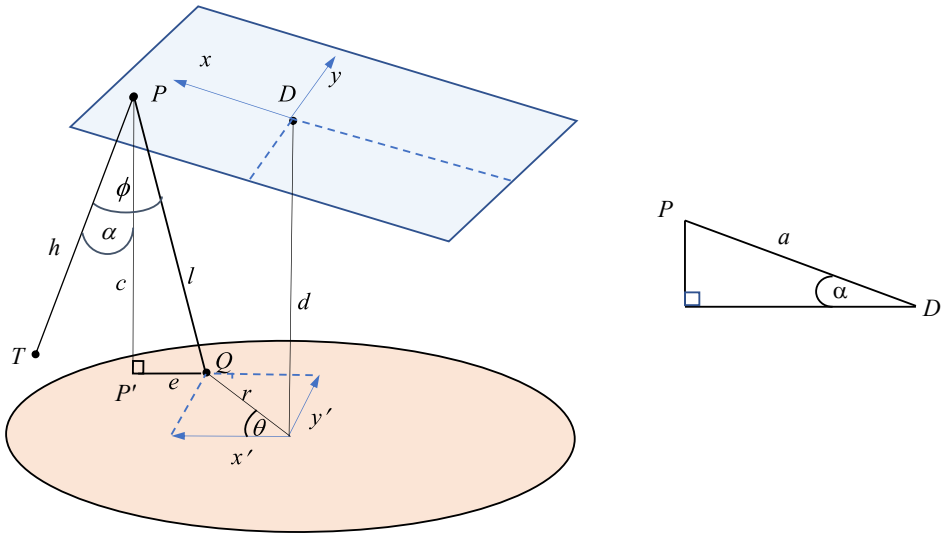

Figure 3. Illustration of distances and angles involved in calculation for points on a square. *Q* is the point on the source surface where the radiation originates, *P* is the point of interest on the square and *P*' is vertically below this. *T* is the point where the normal to the square surface at point *P* crosses the plane of the circle. It can be inside or outside the circle.

The centre of the phantom front face is assumed to be at point *D* at a height *d* vertically above the centre of the circle, and the square may be tilted by an angle α about an axis along the *y* direction on the square. Note *y* is parallel to *y'*, but *x* is not parallel to *x'* except when $\alpha = 0$ when the two planes are parallel. The point *P* on the square is at (*x*,*y*) coordinates (*a*,*b*) on this surface. Its height *c* above the plane of the source is therefore:

$$c = d + a \cdot \sin(\alpha) \tag{8}$$

The distance *l* from the point *P* to a point *Q* on the source area is given by:

$$l = \sqrt{c^2 + e^2} \tag{9}$$

Figure 4 shows points and angles on the surface of the source. Because the tilting of the target surface is about the *y* axis *P'* has coordinates ($a \cdot \cos(\alpha)$, *b*) on the source surface.

The distance *e* can be calculated from:

$$e = \sqrt{(a \cdot \cos(\alpha) - x')^2 + (b - y')^2} \tag{10}$$

The coordinates of point *Q* on the surface source are $x' = r \cdot \cos(\theta)$ and $y' = r \cdot \sin(\theta)$ so that:

$$e = \sqrt{(a \cdot \cos(\alpha) - r \cdot \cos(\theta))^2 + (b - r \cdot \sin(\theta))^2} \tag{11}$$

The fact that $(a\cdot\cos(\alpha)-r\cdot\cos(\theta))$ and $(b-r\cdot\sin(\theta))$ may be negative is not an issue as they are squared in equation (11).

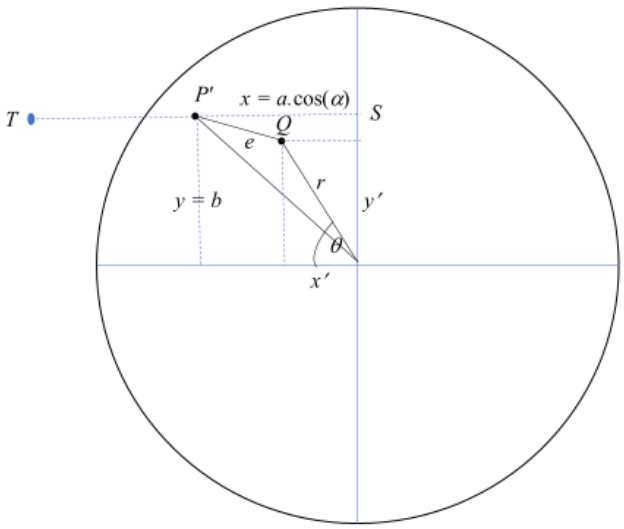

Figure 4. Distances and angles in the plane of the source circle. *P′* is vertically below *P*. *T* is where the normal to the square at point *P* crosses the plane containing the circle. Since the square is only tilted about the *y* axis the line *TP′* is always parallel to the *x′* axis and crosses the *y′* axis at point *S*.

Substituting the values for the components of *l* from equations (9) and (11) into equation (1) the equation for L_a is:

$$L_a=\frac{\int_0^R\int_0^{2\pi}(1/l^2)\cdot r\,\mathrm{d}r\,\mathrm{d}\theta}{\pi R^2}=\frac{\int_0^R\int_0^{2\pi}1/(c^2+e^2)\cdot r\,\mathrm{d}r\,\mathrm{d}\theta}{\pi R^2} \tag{12}$$

Substituting for *c* and *e* from equations (8) and (10), the equation for L_a becomes:

$$L_a=\frac{1}{\pi R^2}\int_0^R\int_0^{2\pi}1/((d+a\cdot\sin(\alpha))^2+(a\cdot\cos(\alpha)-r\cdot\cos(\theta))^2+(b-r\cdot\sin(\theta))^2)\cdot r\,\mathrm{d}r\,\mathrm{d}\theta \tag{13}$$

From Figure 3 the angle of incidence ϕ is obtained from the triangle *TPQ* where:

$$TP=h=c/\cos(\alpha)=(d+a\cdot\sin(\alpha))/\cos(\alpha) \tag{14}$$

and

$$PQ=l=\sqrt{c^2+e^2}=\sqrt{(d+a\cdot\sin(\alpha))^2+(a\cdot\cos(\alpha)-r\cdot\cos(\theta))^2+(b-r\cdot\sin(\theta))^2} \tag{15}$$

and from Figure 4:

$$\begin{aligned}TQ=g&=\sqrt{(TP'+P'S-x')^2+(b-y')^2}\\&=\sqrt{(c\cdot\tan(\alpha)+a\cdot\cos(\alpha)-r\cdot\cos(\theta))^2+(b-r\cdot\sin(\theta))^2}\end{aligned} \tag{16}$$

The angle ϕ is then given by:

$$\cos(\phi) = \frac{(l^2 + h^2 - g^2)}{2 \cdot l \cdot h} \tag{17}$$

The equation for the average angle of incidence ϕ_a for points on the circle is then:

$$\phi_a = \frac{\int_0^R \int_0^{2\pi} \arccos\left(\frac{(l^2 + h^2 - g^2)}{2 \cdot l \cdot h}\right) \cdot r \, \mathrm{d}r \, \mathrm{d}\theta}{\pi R^2} \tag{18}$$

As mentioned in section 2, this is not the best estimate of the average angle of incidence for radiation from the circle. For this the fluence-weighted average angle ϕ_{fwa} is required:

$$\phi_{fwa} = \frac{\int_0^R \int_0^{2\pi} \arccos\left(\frac{(l^2 + h^2 - g^2)}{2 \cdot l \cdot h}\right) / (c^2 + e^2) \cdot r \, \mathrm{d}r \, \mathrm{d}\theta}{L_a \pi R^2} \tag{19}$$

The equation for the average distance is:

$$l_a = \frac{1}{\pi R^2} \int_0^R \int_0^{2\pi} \sqrt{(d + a \cdot \sin(\alpha))^2 + (a \cdot \cos(\alpha) - r \cdot \cos(\theta))^2 + (b - r \cdot \sin(\theta))^2} \cdot r \, \mathrm{d}r \, \mathrm{d}\theta \tag{20}$$

Because several of the parameters are functions of both r and θ the double integrals for the quantities describing the average distances and angles cannot be simplified to a single integral by first performing the integration over angle θ. A Fortran program, called Coldiv, has been written to calculate these double integrals using NAG Library routine D01DAF which performs the evaluation to a specified absolute accuracy by repeated applications of the method described by Patterson (1968) [3] and Patterson (1969) [4]. Details are given in Appendix 1. - The program Coldiv.

These equations are complex so the results for points where the coordinates a and b are 0, i.e. points on the axis through the centre of the circle, were compared with those from the simpler equations for points on this line. Values derived for the three quantities from the Fortran program agreed exactly with the values in Table 1 giving a degree of confidence in the code.

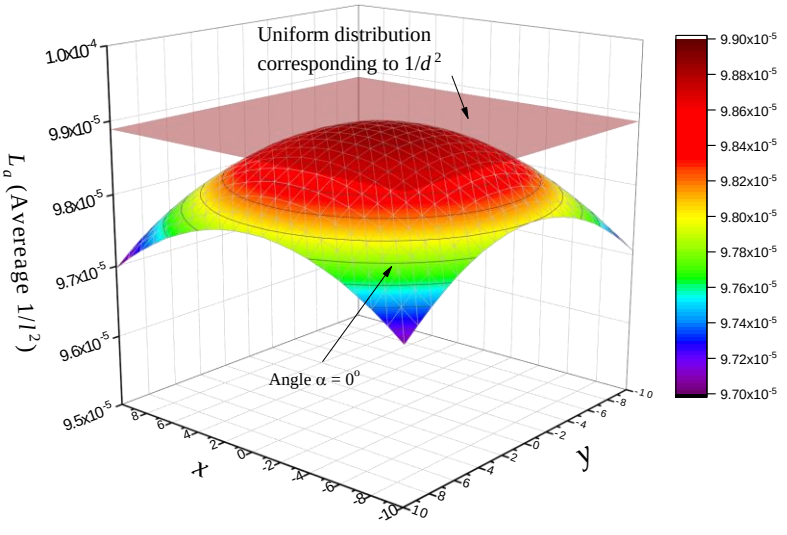

Figure 5. Variation of L_a, the average value of $1/l^2$ for a circle of radius R = 15 for points (x,y) on a 20 × 20 square positioned above the circle and parallel to it at a height d of 100 ($\alpha = 0^o$).

Examples of the results for L_a from Coldiv are presented in Figure 5 for a circle of radius 15 a square of sides 20 × 20, and d = 100 with the square parallel to the plane of the circle.

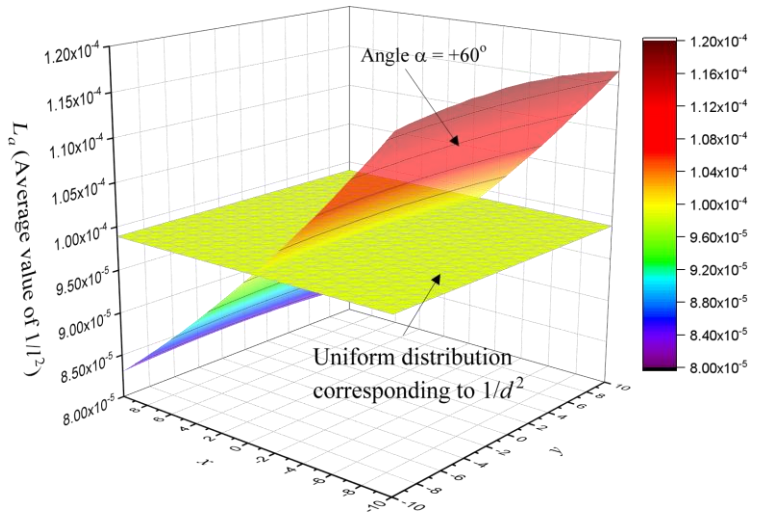

Figure 6. Variation of L_a, the average value of $1/l^2$ for a circle of radius R = 15 for points on a 20 × 20 square with its centre at a height d of 100 above the centre of the circle and with the square tilted by +60° about its y axis.

Figure 6 shows the data for the same configuration but with the square tilted at an angle α of +60° relative to its y axis. The variation of L_a is now very much greater.

The average angle of incidence ϕ_a subtended at a point P above the circular source by points on the circle, and the fluence weighted average angle of incidence for radiation ϕ_{fwa} can be calculated from eq. (18) and eq. (19) respectively.

Data on the difference between these two quantities are presented in

Figure 7, and in Table 2 for points on the axis of the source circle.

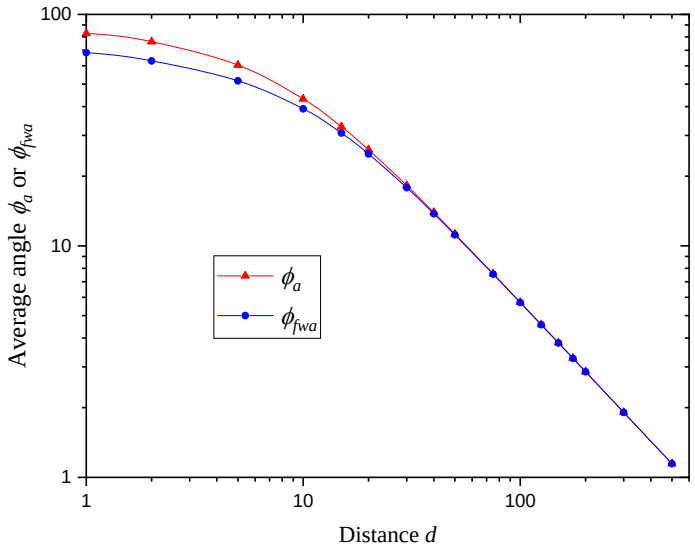

Figure 7. Comparison of the variation of ϕ_a and ϕ_{fwa} with distance d.

Table 2. Difference between average angle ϕ_a and the fluence-weighted average angle ϕ_{fwa} for points on a line perpendicular to the centre of the source circle. The angles range from 0° to ϕ^{max}.

Height above source plane (d)	Average angle ϕ_a	Fluence-weighted average angle ϕ_{fwa}	Difference between ϕ_a and ϕ_{fwa}	Maximum ϕ ϕ^{max}
1	82.75°	68.39°	15.0%	86.19°
2	76.23°	62.92°	21.0%	82.41°
5	60.42°	51.64°	21.2%	71.57°
10	43.14°	39.08°	17.0%	56.31°
15	32.70°	30.71°	10.4%	45.00°
20	26.02°	24.95°	6.48%	36.87°
30	18.23°	17.84°	4.28%	26.57°
40	13.94°	13.76°	2.19%	20.56°
50	11.26°	11.16°	1.30%	16.70°
75	7.58°	7.55°	0.86%	11.31°
100	5.70°	5.69°	0.39%	8.53°
125	4.57°	4.56°	0.22%	6.84°
150	3.81°	3.81°	0.14%	5.71°
175	3.27°	3.27°	0.10%	4.90°
200	2.86°	2.86°	0.070%	4.29°
500	1.15°	1.15°	0.056%	1.72°

As illustrated in both Figure 7 and Table 2, differences between ϕ_a and ϕ_{fwa} are small at the distances where device irradiations are usually performed, i.e. 100 cm to 200 cm. Nevertheless, as ϕ_{fwa} is the better estimate of the average angle of incidence for radiation, all angle data presented subsequently are for ϕ_{fwa}.

Examples of the variation of the fluence weighted average incidence angle ϕ_{fwa} for points on a 20 × 20 square positioned at a distance of 100 above the circular source of radius 15 are shown in Figure 8 for the square parallel to the plane of the circle, and in Figure 9 for the square tilted by 60º.

As can be seen from Figure 8, and as listed in Table 2, even at (x = 0, y = 0) and a tilt angle α = 0° the average angle of incidence ϕ_{fwa} is 5.69º. (This is reasonable since ϕ varies between 0º and 8.5º and the larger angles contribute more because the area on the source increases as r increases.) From the data of Figure 5 the fluence at the corners of a 20 × 20 square is about 1.9% less than at the centre, but the fluence weighted average angle, ϕ_{fwa}, is 9.12º compared to 5.69º at the centre. An increase of 60%, a much bigger percentage change.

On increasing the angle α the range of average angles ϕ_{fwa} for points on the square increases. For example, for the configuration of Figure 9, i.e. R = 15, d = 100, and α = 60º, ϕ_{fwa} = 57.0º for x = -10, y = 0 and ϕ_{fwa} = 62.7º for x =10, y =0, a 10% change. The variation in the fluence is greater varying from 1.18×10^{-4} at x = -10, y = 0 to 8.37×10^{-5} at x = 10, y =0, a 41% change.

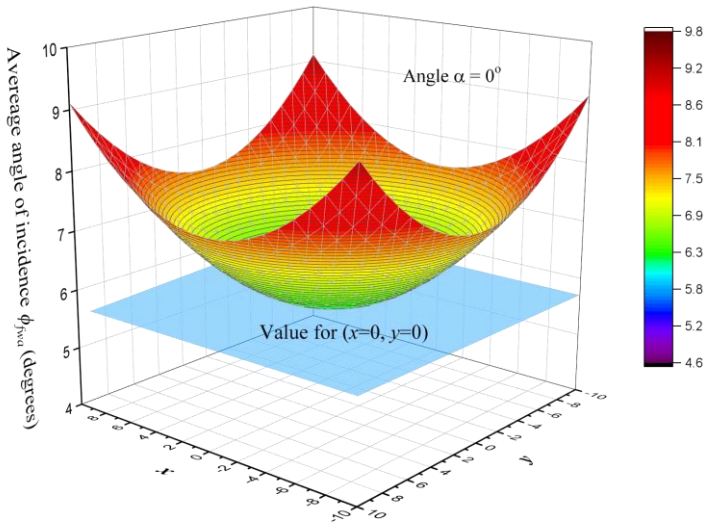

Figure 8. Variation of the average angle of incidence ϕ_{fwa} with position on a 20 × 20 square at a height of 100 above a circular source of radius 15 when the square and circle parallel to each other (α=0°).

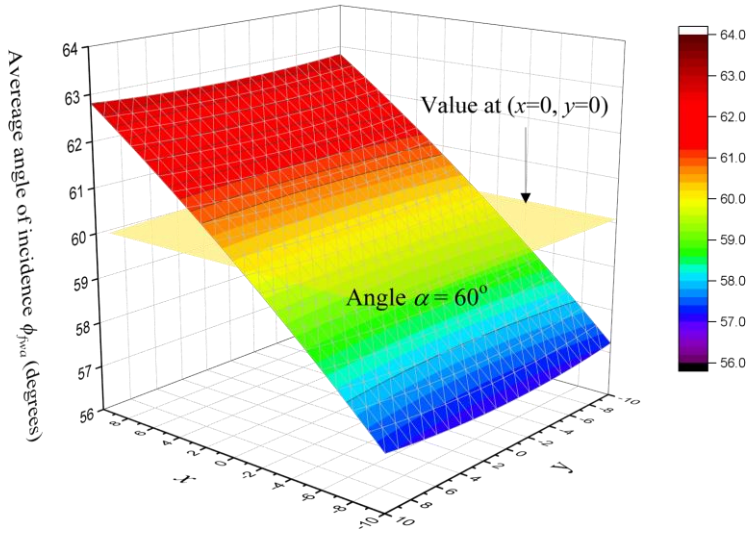

Figure 9. Variation of the average angle of incidence ϕ_a with position on a 20 × 20 square above a circular source of radius 15 when the centre of the square is at a height of 100 above the circle and the x axis of the square is tilted at an angle α=60° relative to the plane of the circle.

For a point at the centre of the square, i.e. on the normal through the centre of the source circle, the average angle of incidence ϕ_{fwa} approaches the value of α as α increases. The values of ϕ_{fwa} are shown in Table 3 for R = 15 and d = 100. For a 90° tilt the average angle of incidence is 90° although this is just a result of the symmetry of the arrangement at this tilt angle, the actual angles varying between roughly 81.5° and 98.5°. This means that irradiations of personal dosemeters on a phantom cannot be performed for this angle. However, the requirement for thermal irradiation of dosemeters through their sides [5] is for an irradiation at 85°. (This is a test for shielding of the sensitive elements in albedo neutron detectors from direct thermal neutrons.) For this type of irradiation the distance d must exceed 170.

Table 3. Average fluence-weighted incidence angle
for the centre of the square for R=15, d=100

Tilt angle α	Average incidence angle ϕ_{fwa}	Minimum incidence angle	Maximum incidence angle
0°	5.70°	0°	8.53°
5°	7.13°	0°	13.53°
10°	10.94°	1.47°	18.53°
15°	15.61°	6.47°	23.53°
20°	20.44°	11.47°	28.53°
30°	30.28°	21.47°	38.53°
45°	45.16°	36.47°	53.53°
60°	60.09°	51.47°	68.53°
75°	75.04°	66.47°	83.53°
85°	85.01°	76.47°	93.53°
90°	90.00°	81.47°	98.53°

4. Corrections for the fluence and angle variations

The program Coldiv calculates the radiation fluence at points on a rectangular surface above a uniform spherical disk source, relative to the fluence at the point where the normal through the centre of the source crosses the rectangular surface. More precisely it calculates the inverse of the square of the average distance from points on the circle to the point of interest on the rectangle which is a measure of the fluence. The fluence-weighted average angle of incidence is also calculated. The program's main use is to calculate these quantities for points on a rectangular surface (usually the surface of a phantom) on which personal dosemeters are placed for calibration in the thermal neutron beam of the column on the NPL thermal pile. (As the thermal column is a 30 cm diameter, 1 m or 1.5 m long, cadmium-lined tube, the program only provides valid results for a circular area of 30 cm diameter above the column, but this is not a drawback for most layouts where the dosemeters are arranged within a 20 × 20 cm^2 square.)

The thermal neutron fluence is calibrated at a point on the central axis of the column via the activation of small gold foils, 1 cm^2 in area, placed at this position. Coldiv allows corrections to this fluence value to be made for off-axis points where the sensitive elements of neutron dosemeters may be located and the average distance from points on the source is greater.

Personal dosemeters are calibrated in terms of personal dose equivalent, a quantity that depends on the angle of incidence on the dosemeter. With a circular radiation source any dosemeter sees neutrons incident with a range of angles. The column is quite long compared to its diameter, so the range of angles is reasonably small but, as indicated in Table 3, the fluence-weighted average angle for a point on the axis of the cylinder at 1 m from the source is 5.69°. The possible angles of incidence range from -8.53°. To +8.53°.

Calibration requests usually specify particular incidence angles, usually 0°, 30°, or 60° since these are the ones specified in the ISO standard for calibration of personal dosemeters [(5)]. Because of the divergence of the column beam calibrations at precisely these angles are not possible. By increasing the distance in the column the divergence can be decreased, for example the fluence-weighted average angles on the column axis are 3.81° at 150 cm and 2.86°

at 200 cm. However, the fluence decreases as the distance increases meaning calibrations of low-efficiency personal dosemeters take longer when the distance is large.

Values for personal dose equivalent for neutrons are derived by multiplying the fluence by fluence to personal dose equivalent conversion coefficients [6], and these have both an energy and an angular dependence. The angular variations of these coefficients, for energies around the thermal region, are shown in Figure 10. There are curves for 10 meV, 25.3 meV, and 100 meV. The idealised thermal neutron distribution is a Maxwellian with a temperature of 20.4°C (nominal room temperature). This peaks at 25.3 meV, but the mean neutron energy is twice this value, i.e. 50.6 meV.

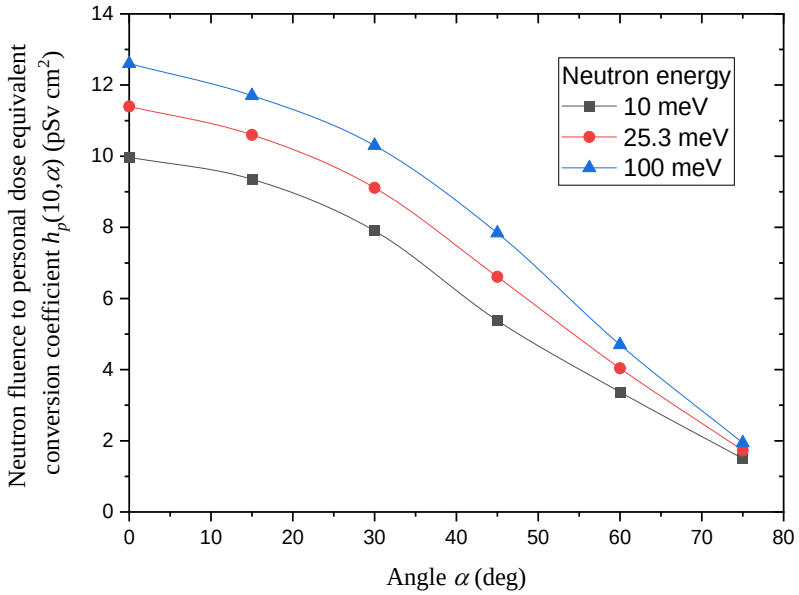

Figure 10. Neutron fluence to personal dose equivalent conversion coefficients, $h_p(10,\alpha)$, as a function of angle of incidence for energies in the thermal region.

The derivation of an appropriate set of conversion coefficients for a particular thermal field requires the conversion coefficients to be averaged over the neutron spectrum which, because of incomplete thermalisation, will rarely be an idealised Maxwellian at 20.4°C. This averaging has been done for the NPL thermal column field using the available spectral information giving values for incidence at 0°, 30°, and 60° [7]. These need to be corrected for the spread of the angles in the actual experimental configuration.

Fortunately the curves for $h_p(10,\alpha)$, illustrated in Figure 10, run reasonably parallel to each other in the thermal region so an adequate estimate of the percentage deviation of the conversion coefficients from the values for 0°, 30°, and 60° can be derived from the curve for 25.3 meV. Since there is no obvious functional form that fits the variation over the full energy range, values for the conversion coefficients were determined by fitting the three nearest points to the angle of interest to a quadratic, and the value for angles in a particular range derived from the fitted quadratic. Thus, for angles around 0° the data fitted was for 0°, 15°, and 30°, for angles around 30° the data fitted was for 15°, 30°, and 45°, for angles around 60° the data fitted was that at 45°, 60° and 75°. As an example, the change in the conversion coefficient in going from 0° to 5.69°, the latter number being the fluence-weighted average angle on the column axis at 100 cm, is -2.0 %. The corresponding number for 150 cm, where the fluence-weighted average angle is 3.81°, is -1.2 % and at 200 cm the numbers are 2.86° and -0.9 %.

Performing a detailed analysis of the variation of the personal dose equivalent with dosemeter position is a lengthy process and often offers only limited improvement in accuracy. Therefore,

it must be decided for each dosemeter calibration whether this process is warranted. Coldiv provides information both for making this choice, and for performing the corrections if they are deemed necessary.

Appendix 2 contains tables of data for the three most commonly used heights in the thermal column, i.e. 100 cm, 150 cm, and 200 cm. At each height there are data sets for a plane perpendicular to the source circle, i.e. a 0° tilt, one at a tilt angle of 30° to this circle, and one for a tilt angle of 60°. Each Coldiv calculation provided data for 121 points, an 11 by 11 matrix, distributed evenly over a 20×20 cm^2 square. The quantities given for each point are: the fluence-weighted average angle, the percentage differences in the value of the fluence to personal dose equivalent conversion coefficient, $h_p(10,\alpha)$, and the percentage difference in the fluences. The percentage differences in $h_p(10,\alpha)$ are relative to the value at the nominal angles, i.e. 0°, 30°, 60°. They allow for the divergence of the field and are thus not zero, even on a line along the axis of the source.

For a tilt angle of 0° the four quadrants of the square are symmetric so each quantity in this configuration only contains 36 numbers; these are shown in Tables A1 to A3. For tilt angles of 30° and 60° there is symmetry about the $y = 0$ line so these tables, i.e. Table A4 to A9, contain 66 numbers for each quantity.

Coldiv can be run to determine corrections for any dosemeter configuration, and this should be done when there is uncertainty about the magnitude of these corrections. The tables in Appendix 2 provide useful information for some standard configurations. Table 4 shows data for points on a plane parallel to the source with two configurations considered, a single dosemeter at the point ($x = 0$, $y = 0$) on the axis of the circular source, and points distributed over a 20×20 cm^2 square. These are based on data from Tables A1 to A3.

For a single dosemeter at point ($x = 0$, $y = 0$) reductions in the personal dose equivalent delivered, compared to that calculated assuming 0° incidence, arise because of the range of incident angles. The range of distances does not need to be taken into consideration because the fluence is measured by a gold foil at ($x = 0$, $y = 0$). Table 4 gives values for the corrections (reductions) in $h_p(10,\alpha)$ derived from a comparison of the value for the fluence-weighted average angle of incidence compared to that for the reference value for 0° incidence. The size of the correction decreases as the height increases going from -2.0% at 100 cm to -0.9% at 200 cm. The uncertainties are a simple estimate of possible inaccuracies in the calculations.

Table 4. Estimates of corrections to the personal dose equivalent derived from a measurement of the fluence at the reference position ($x = 0$, $y = 0$) for two possible configurations of dosemeters on a surface parallel to a 15 cm diameter surface source.

Distance (cm)	One dosemeter at ($x = 0$, $y = 0$)	Dosemeters distributed over a 20×20 cm^2 area centred on the source central axis	
	Correction to $h_p(10,\alpha)$ for the average angle	Average value of fluence reductions	Correction to $h_p(10,\alpha)$ average over all angles
100	(-2.0 ± 0.5) %	(-1.0 ± 1.0)%	(-2.8 ± 0.8) %
150	(-1.2 ± 0.5) %	(-0.5 ± 0.5)%	(-1.7 ± 0.5) %
200	(-0.9 ± 0.5) %	(-0.3 ± 0.3)%	(-1.2 ± 0.3) %

For dosemeters evenly distributed over a 20×20 cm^2 square area corrections are required for the increased average distance as well as the range of incidence angles. For a distance of 100 cm the effects of different average distances from points on the circle to those on the square vary from 0 % at ($x = 0$, $y = 0$) to almost -2 % at the corners. An average decrease of (-1.0 ± 1.0) % in the fluence could thus be used to allow for this effect. Similarly the reduction in $h_p(10,\alpha)$ varies from -2.0 % at ($x = 0$, $y = 0$) to -3.5 % at the corners. A correction of (-2.8 ± 0.8) % could thus be used to allow for this effect.

In view of the typical uncertainties in personal dosemeter calibrations a single correction factors for all dosemeter when they are distributed over a 20×20 cm^2 square should be acceptable, rather than trying to calculate corrections for each dosemeter position separately. For irradiations with the dosemeters on a surface angled at 30° or 60° the application of average correction factors to all the dosemeters, for both the change of the fluence, and the fluence to dose equivalent conversion coefficient, with position on the surface is not feasible. For a distance of 100 cm to the tilted surface along the normal from the centre of the source disc, and a tilt angle of 60°, the differences in the personal dose equivalent conversion coefficient compared to the value for exactly 60° incidence are (see Table A7): -0.4 % at ($x = 0$, $y = 0$), 12.0 % at ($x = -10$, $y = 0$), and -11.1 % for ($x = 10$, $y = 10$). (The value of -0.4 % at ($x = 0$, $y = 0$) is actually less than the value of -2.0 % for a tilt angle of 0°. This is because the angles for 0° tilt vary from 0° to 8.53° i.e. are all ≥0°, whereas, at a tilt angle of 60°, the angles of incidence can be less than or greater than 60°.) The variations in the fluence corrections are even larger with values of: 0 % at ($x = 0$, $y = 0$), 19.3 % at ($x = -10$, $y = 0$), and -16.0 % for ($x = 10$, $y = 10$). These are far too large to consider using average values for the fluence or $h_p(10,\alpha)$ corrections.

The alternative to calculating correction factors for each dosemeter position is to only position the dosemeters along the $x = 0$ line. The changes along this line are small, and the corrections that have to be applied to the reference value derived for 0° incidence at $x = 0$, $y = 0$ to cover these are listed in Table 5 as derived from Tables A4 to A9.

Table 5. Estimates of corrections that need to be applied to the personal dose equivalent derived for 0° incidence at $x = 0$, $y = 0$ for dosemeters distributed along the $x = 0$ line for tilt angles of 30° or 60° (they are essentially the same) and for three heights.

Distance (cm)	One dosemeter at ($x = 0$, $y = 0$)	Dosemeters distributed over range from $y = -10$ cm to +10 cm	
	Angle correction	Distance correction	Angle correction
100	(-0.4 ± 0.1)%	(-0.5 ± 0.5)%	(-0.8 ± 0.4)%
150	(-0.2 ± 0.1)%	(-0.2 ± 0.2)%	(-0.4 ± 0.2)%
200	(-0.1 ± 0.1)%	(-0.1 ± 0.1)%	(-0.2 ± 0.1)%

The question of whether additional rows with small values of x could also be used, depending on the dosemeter size, could be answered by running Coldiv for specific configurations of x and y values.

5. Validation of the calculations and comparison with experiment

As explained in Section 3 the data from the numerical integration program Coldiv for points on the central axis of the source disc were checked against the analytical calculations in Section 2. However, for off-axis points, this is not possible. To check the off-axis results a Monte Carlo

code which had been written to calculate average fluences and angles of incidence over a circular target area at a distance from a circular source was modified and run using a number of target points at selected positions and tilt angles. These gave exact agreement with Coldiv. This is not a check that the equations outlined in Section 3 are correct, but it does validate the NAG library approach for numerical integration.

Coldiv predicts that, despite the source being 30 cm in diameter, the decrease in the fluence with height in the column can be reasonably accurately described by an inverse square law dependence on the distance from the source, for distances above 100 cm. Several experiments over the years have demonstrated this dependence. Figure 11 shows data obtained using a small, 6 cm long 1.2 cm diameter, BF_3 proportional counter tube. The BF_3 counts have been divided by the reading of the fission chamber (FC) located near the bottom of the column which is the usual monitor for irradiations of devices in the column beam.

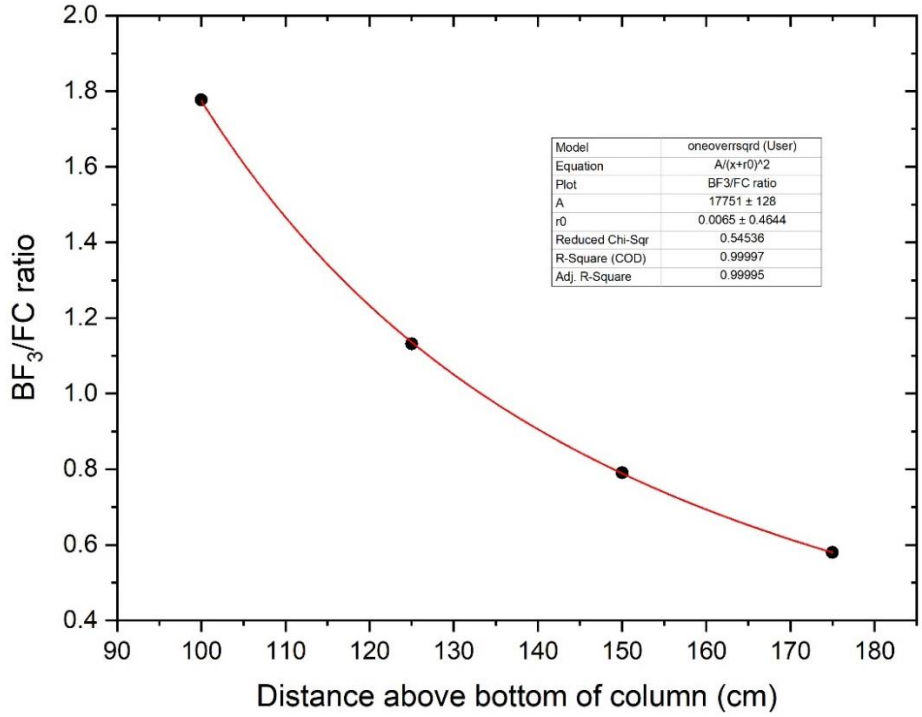

Figure 11. BF_3 proportional counter measurements of the height dependence of the neutron fluence in the thermal column

The data have been fitted to the function $A/(x+r_0)^2$ where x is the measured distance and r_0 is a measure of any deviation of zero on the x scale from the actual position of the source area at the bottom of the column. The quantity A is the ratio at $x = r_0$ and has a large uncertainty. This is linked to the large uncertainty in the quantity r_0 which is essentially zero within the uncertainties.

Another quantity that Coldiv predicts that can be checked against experiment is the variation of the fluence across the thermal column beam. Figure 12 shows a comparison of the calculated data with measurements performed with gold foils at the 1 m height in the column.

The uncertainties in the gold foil measurements are unfortunately quite large when viewing effects of the order of 2 %, but there is clear agreement between the measured and calculated data. The measured results were fitted to a parabola, and this is also plotted on the graph and shows a very similar variation with distance from the column central axis to the calculated data.

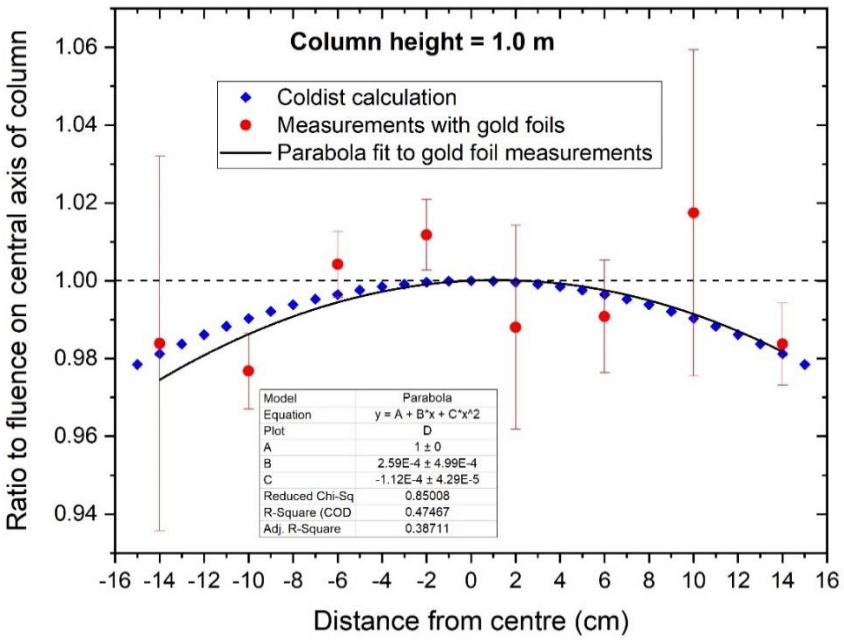

Figure 12. Comparison of the variation of the fluence across the thermal column beam as calculated with Coldiv against activation measurements with gold foils.

Data for other heights in the column do not display quite as good agreement between measurement and calculation. Figure 13 shows a comparison of Coldiv data with historical measurements taken with a small BF_3 proportional counter. This was the same BF_3 counter as was used to obtain the data shown in Figure 11. Results were taken both along the direction of the deuteron beam that produces the neutrons by reaction with beryllium targets within the pile, and also across this direction. These measurement sets agree well with each other.

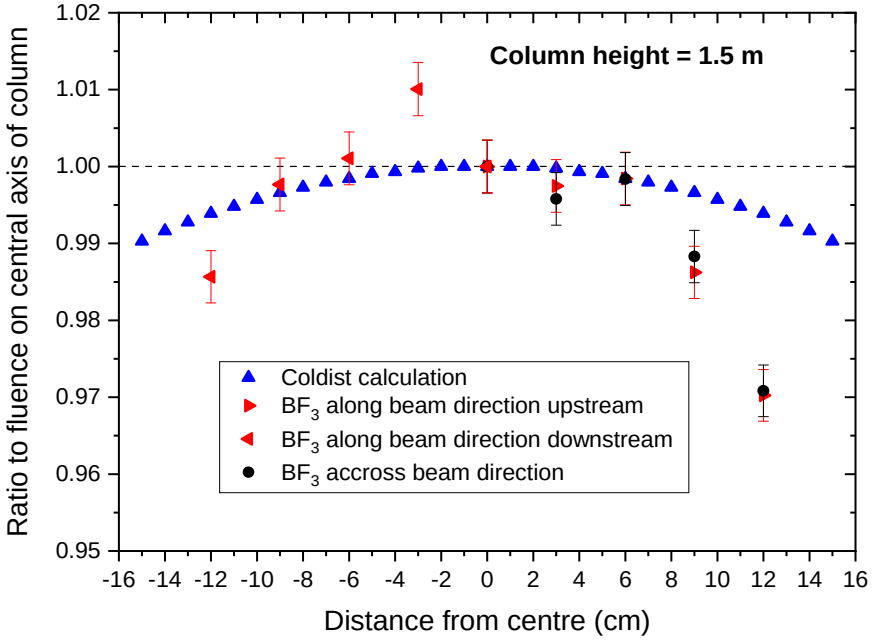

Figure 13. Comparison of the variation of the fluence across the thermal column beam as calculated with Coldiv against measurements with a small BF_3 proportional counter

The reasons for the discrepancies are not clear. The BF_3 counter has an active length of 6 cm which might affect the results. However, a comparison of the ratios of fluences calculated using Coldiv at various distances to those on the central axis of the column were not changed when averages were taken over lines of length 6 cm. These measurements need to be repeated.

6. Conclusions

A number of issues, resulting from the neutron source at the bottom of the thermal column being a disc of radius 15 cm, have an influence on quantities quoted in NPL certificates for thermal neutron irradiation. These have not been thoroughly investigated in the past, the assumption made was that they were negligible. They have been investigated here and the effects quantified.

A small Fortran program, Coldiv, was written to perform the investigation and the results that emerged are listed below.

a) The decrease in the field intensity as the distance between source and measurement point increases, depends of course on the source radius and the actual distance from the source, but the decrease exhibits an inverse square law dependence for distances in excess of 100 when the source has a radius of 15. The validity of this approximation for any other source radius can easily be checked with Coldiv.

b) For a measuring device with a response that depends on the angle of incidence, allowance should be made for the divergence of the field. For example, when performing personal dosemeter calibrations in the NPL thermal pile a correction of about 2% to the personal dose equivalent delivered needs to be made even for a single dosemeter on the axis of the disc source.

c) For the irradiation of a set of personal dosemeters covering an area of about 20×20 cm^2 on a flat surface normal to the axis of the source average corrections can still be made although the uncertainty increases.

d) If irradiations of personal dosemeters at angles other than normal incidence need to be made, the variation of the dose with position on a tilted flat surface are too large to allow average corrections to be made. The best approach is to arrange the personal dosemeters in a line along the tilt axis. If the dosemeters are spread out over the surface corrections need to be calculated for each dosemeter separately. Coldiv can do this, but it involves a considerable increase in the time and effort to perform calibrations. It also means each dosemeter is irradiated in a different field which may be something the customer would not want.

Acknowledgements

This work was supported by the National Measurement System of the UK government's Department for Science, Innovation and Technology. Matt Birch's demonstration of how easily a simple Monte Carlo code can be written is gratefully acknowledged.

References

1 International Organization for Standardization, *Reference radiation fields for radiation protection — Definitions and fundamental concepts*, International Standard ISO 29661, 2012

2 N.P. Hawkes, et al., *Additional Characterisation of the Thermal Neutron Pile at the National Physical Laboratory, UK*, Rad. Prot. Dosim., **180**, No. 1–4, (2018) 25–28.

3 T.N.L. Patterson, *On some Gauss and Lobatto based integration formulae*, Math. Comput. **22** (1968) 877–881.

4 T.N.L. Patterson, *The optimum addition of points to quadrature formulae, errata*, Math. Comput. (1969) 892.

5 International Organization for Standardization, *Passive neutron dosimetry systems — Part 1: Performance and test requirements for personal dosimetry*, International Standard ISO 21909-1 2015.

6 *Conversion coefficients for use in Radiological Protection Against External Radiation*, results of a joint ICRP/ICRU task group, published by the International Commission on Radiological Protection as ICRP Publication 74, 1996, and by the International Commission on Radiation Units and Measurements as ICRU Report 57, 1998.

7 David J. Thomas and Peter Kolkowski, *Thermal fluence and dose equivalent standards at NPL*, NPL Report RN008, March 2005.

7. Appendix 1. - The program Coldiv

Coldiv calculates the average distances l_a, the average angle ϕ_a, the fluence weighted average angle ϕ_{fwa}, and the average, L_a, of $1/l^2$, for a set of x and y points (a,b) on a square positioned at a distance d from a circular radiation source.

Inputs to the program are provided in the file Coldivin.dat and are:

absacc	a value for the absolute accuracy required by the NAG integral routine D01DAF
R	the radius of the circle
nd	the number of different distances (maximum 20)
distances	*nd* values for the required distances separated by a space
pm	M (or m) for a matrix of points on the square, P (or p) to input points as *x*,*y* pairs
If *pm*=M:	
side	the length of the sides of the square
na and *nb*	the number of x and y distances respectively on the square (maximum 50 points)
If *pm*=P:	
np	number of pairs of points
(a_i, b_i)	*np* pairs of x and y coordinates one pair per line (maximum 50 points)
α	the angle in degrees by which the square is tilted about its $x = 0$ axis.
calang	set to Y (or y) to calculate the average angle (see reason outlined below for including this option).
pout	this is a debugging feature - set to a, b, c, or d to print out the parameters used when calculating the average distance, the average angle, the fluence-weighted average angle, or the average $1/\text{dist}^2$ respectively. Use any other character for no printing. Output is to a file Coldbug.dat

Output from the program is to the file Coldivou.dat

The program, an input data file Coldiv.dat with typical inputs, and a batch file, RunCold, for running the program can be found at:
T:\NUCLEAR\Technical\Software\Neutrons\Coldiv_NAG\

Coldiv was assembled by modifying the example program given in the NAG library for using the routine D01DAFD. The value used in the example for absacc is 1×10^{-6}. Calculations for l_a, the fluence-weighted average angle, ϕ_{fwa}, and the average of $1/l^2$ converge for this value of absacc for all cases tried, but the calculations for ϕ_a did not always do so depending on the points (a,b) and the distance d. In fact, absacc had to be reduced significantly, e.g. to 0.02 in some cases, to achieve convergence. The reason for this is not clear. The value of ϕ varies smoothly with r and θ so the failure to converge is surprising. This problem casts an element of doubt on the accuracy off the calculation of ϕ_a. The approach taken to minimise any error was to find the smallest absacc for which convergence is achieved and compare the answers with those obtained for larger absacc values. Ultimately, however, the most useful average angle is the fluence-weighted one, ϕ_{fwa}, and the program does not tend to fail for this quantity even for small values of absacc around.

Using the option (cang = N or n) of not calculating the average angle of incidence allows absacc to be set at 1×10^{-6} for calculating l_a and L_a the average of $1/l^2$. The values of l_a and the average of *La* change very little and in most cases not at all as absacc is reduced below 0.02.

The Monte Carlo version of the program, ColdivMC, can be found at:
Z:\NUCLEAR\Technical\Software\Neutrons\Coldiv_MC\
Because it relies on the use of large random number lists the program is slow so is written to calculate for only one point (*a*,*b*) at a time. A sample input file, ColdivMC.inp, with annotation in the file explaining each input datum, and a batch file RunColdMC.BAT are available for running the program. Output is to a file ColdiMC.out.

8. Appendix 2. – Data for three commonly used heights in the NPL thermal column

Table A 1. Percentage differences for fluence weighted angles, fluence to $h_p(10,\alpha)$ conversion coefficients, and fluences, for distance d = 100 and tilt angle $\alpha = 0°$ for positions with a range of (x,y) coordinates, on a rectangular plane above a circular source of radius 15.

Fluence-weighted average angles, ϕ_{fwa} (degrees)						
	x = 0	x = 2	x = 4	x = 6	x = 8	x = 10
y = 0	5.69	5.76	5.98	6.34	6.84	7.46
y = 2	5.76	5.84	6.05	6.41	6.91	7.53
y = 4	5.98	6.05	6.27	6.62	7.12	7.73
y = 6	6.34	6.41	6.62	6.98	7.46	8.07
y = 8	6.84	6.91	7.12	7.46	7.94	8.53
y = 10	7.46	7.53	7.73	8.07	8.53	9.11

$h_p(10,\alpha)$, difference to value for angle of incidence = 0°						
	x = 0	x = 2	x = 4	x = 6	x = 8	x = 10
y = 0	-2.0%	-2.0%	-2.1%	-2.2%	-2.4%	-2.7%
y = 2	-2.0%	-2.0%	-2.1%	-2.3%	-2.5%	-2.8%
y = 4	-2.1%	-2.1%	-2.2%	-2.4%	-2.6%	-2.9%
y = 6	-2.2%	-2.3%	-2.4%	-2.5%	-2.7%	-3.0%
y = 8	-2.4%	-2.5%	-2.6%	-2.7%	-3.0%	-3.3%
y = 10	-2.7%	-2.8%	-2.9%	-3.0%	-3.3%	-3.5%

Fluence, difference to value at (x = 0, y = 0)						
	x = 0	x = 2	x = 4	x = 6	x = 8	x = 10
y = 0	0.0%	0.0%	-0.2%	-0.3%	-0.6%	-1.0%
y = 2	0.0%	-0.1%	-0.2%	-0.4%	-0.7%	-1.0%
y = 4	-0.2%	-0.2%	-0.3%	-0.5%	-0.8%	-1.1%
y = 6	-0.3%	-0.4%	-0.5%	-0.7%	-1.0%	-1.3%
y = 8	-0.6%	-0.7%	-0.8%	-1.0%	-1.2%	-1.6%
y = 10	-1.0%	-1.0%	-1.1%	-1.3%	-1.6%	-1.9%

Table A 2. Percentage differences for fluence weighted angles, fluence to $h_p(10,\alpha)$ conversion coefficients, and fluences, for distance d = 150 and tilt angle α = 0° for positions with a range of (x,y) coordinates, on a rectangular plane above a circular source of radius 15.

Fluence-weighted average angles, ϕ_{fwa} (degrees)						
	x = 0	x = 2	x = 4	x = 6	x = 8	x = 10
y = 0	3.81	3.86	4.01	4.25	4.59	5.02
y = 2	3.86	3.91	4.06	4.30	4.64	5.07
y = 4	4.01	4.06	4.20	4.45	4.78	5.21
y = 6	4.25	4.30	4.45	4.69	5.02	5.44
y = 8	4.59	4.64	4.78	5.02	5.34	5.75
y = 10	5.02	5.07	5.21	5.44	5.76	6.15

$h_p(10,\alpha)$, difference to value for angle of incidence = 0°						
	x = 0	x = 2	x = 4	x = 6	x = 8	x = 10
y = 0	-1.2%	-1.2%	-1.3%	-1.4%	-1.5%	-1.7%
y = 2	-1.2%	-1.2%	-1.3%	-1.4%	-1.5%	-1.7%
y = 4	-1.3%	-1.3%	-1.4%	-1.4%	-1.6%	-1.7%
y = 6	-1.4%	-1.4%	-1.5%	-1.5%	-1.7%	-1.8%
y = 8	-1.5%	-1.5%	-1.6%	-1.7%	-1.8%	-2.0%
y = 10	-1.7%	-1.7%	-1.7%	-1.8%	-2.0%	-2.1%

Fluence, difference to value at (x = 0, y = 0)						
	x = 0	x = 2	x = 4	x = 6	x = 8	x = 10
y = 0	0.0%	0.0%	-0.1%	-0.2%	-0.3%	-0.4%
y = 2	0.0%	0.0%	-0.1%	-0.2%	-0.3%	-0.5%
y = 4	-0.1%	-0.1%	-0.1%	-0.2%	-0.4%	-0.5%
y = 6	-0.2%	-0.2%	-0.2%	-0.3%	-0.4%	-0.6%
y = 8	-0.3%	-0.3%	-0.4%	-0.4%	-0.6%	-0.7%
y = 10	-0.4%	-0.5%	-0.5%	-0.6%	-0.7%	-0.9%

Table A 3. Percentage differences for fluence weighted angles, fluence to $h_p(10,\alpha)$ conversion coefficients, and fluences, for distance d = 200 and tilt angle α = 0° for positions with a range of (x,y) coordinates, on a rectangular plane above a circular source of radius 15.

Fluence-weighted average angles, ϕ_{fwa} (degrees)						
	x = 0	x = 2	x = 4	x = 6	x = 8	x = 10
y = 0	2.86	2.90	3.01	3.20	3.45	3.78
y = 2	2.90	2.94	3.05	3.23	3.49	3.81
y = 4	3.01	3.05	3.16	3.34	3.60	3.92
y = 6	3.20	3.23	3.35	3.53	3.78	4.09
y = 8	3.45	3.49	3.60	3.78	4.02	4.33
y = 10	3.78	3.81	3.92	4.10	4.34	4.63

$h_p(10,\alpha)$, difference to value for angle of incidence = 0° degrees						
	x = 0	x = 2	x = 4	x = 6	x = 8	x = 10
y = 0	-0.9%	-0.9%	-0.9%	-1.0%	-1.1%	-1.2%
y = 2	-0.9%	-0.9%	-0.9%	-1.0%	-1.1%	-1.2%
y = 4	-0.9%	-0.9%	-1.0%	-1.0%	-1.1%	-1.2%
y = 6	-1.0%	-1.0%	-1.0%	-1.1%	-1.2%	-1.3%
y = 8	-1.1%	-1.1%	-1.1%	-1.2%	-1.3%	-1.4%
y = 10	-1.2%	-1.2%	-1.2%	-1.3%	-1.4%	-1.5%

Fluence, difference to value at (x = 0, y = 0)						
	x = 0	x = 2	x = 4	x = 6	x = 8	x = 10
y = 0	0.0%	0.0%	0.0%	-0.1%	-0.2%	-0.2%
y = 2	0.0%	0.0%	0.0%	-0.1%	-0.2%	-0.3%
y = 4	0.0%	0.0%	-0.1%	-0.1%	-0.2%	-0.3%
y = 6	-0.1%	-0.1%	-0.1%	-0.2%	-0.2%	-0.3%
y = 8	-0.2%	-0.2%	-0.2%	-0.2%	-0.3%	-0.4%
y = 10	-0.2%	-0.3%	-0.3%	-0.3%	-0.4%	-0.5%

Table A 4. Percentage differences for fluence-weighted angles, fluence to $h_p(10,\alpha)$ conversion coefficients, and fluences, for distance d = 100 and tilt angle α = 30° for positions with a range of (x,y) coordinates, on a rectangular plane above a circular source of radius 15.

Fluence-weighted average angles, ϕ_{fwa} (degrees)											
	x=-10	x=-8	x=-6	x=-4	x=-2	x=0	x=2	x=4	x=6	x=8	x=10
y=0	25.26	26.30	27.32	28.34	29.31	30.28	31.23	32.16	33.08	33.97	34.85
y=2	25.29	26.32	27.34	28.41	29.33	30.30	31.25	32.18	33.09	33.99	34.87
y=4	25.36	26.39	27.41	28.51	29.39	30.35	31.30	32.23	33.14	34.03	34.91
y=6	25.49	26.51	27.52	28.66	29.49	30.45	31.39	32.31	33.22	34.11	34.98
y=8	25.66	26.68	27.67	28.84	29.62	30.57	31.51	32.43	33.33	34.21	35.08
y=10	25.88	26.88	27.87	29.80	29.80	30.74	31.67	32.57	33.47	34.35	35.21

$h_p(10,\alpha)$, difference to value for angle of incidence = 30°											
	x=-10	x=-8	x=-6	x=-4	x=-2	x=0	x=2	x=4	x=6	x=8	x=10
y=0	6.4%	5.1%	3.7%	2.4%	1.0%	-0.4%	-1.8%	-3.3%	-4.7%	-6.2%	-7.7%
y=2	6.3%	5.0%	3.7%	2.3%	1.0%	-0.4%	-1.9%	-3.3%	-4.7%	-6.2%	-7.7%
y=4	6.2%	4.9%	3.6%	2.1%	0.9%	-0.5%	-1.9%	-3.4%	-4.8%	-6.3%	-7.8%
y=6	6.1%	4.8%	3.5%	1.9%	0.7%	-0.7%	-2.1%	-3.5%	-5.0%	-6.4%	-7.9%
y=8	5.9%	4.6%	3.3%	1.7%	0.5%	-0.8%	-2.3%	-3.7%	-5.1%	-6.6%	-8.1%
y=10	5.6%	4.3%	3.0%	0.3%	0.3%	-1.1%	-2.5%	-3.9%	-5.4%	-6.8%	-8.3%

Fluence, difference to value at (x = 0, y = 0)											
	x=-10	x=-8	x=-6	x=-4	x=-2	x=0	x=2	x=4	x=6	x=8	x=10
y=0	9.8%	7.9%	5.9%	4.0%	2.0%	0.0%	-2.0%	-3.9%	-5.9%	-7.9%	-9.8%
y=2	9.7%	7.8%	5.9%	3.9%	1.9%	0.0%	-2.0%	-4.0%	-5.9%	-7.9%	-9.8%
y=4	9.6%	7.7%	5.7%	3.8%	1.8%	-0.2%	-2.1%	-4.1%	-6.1%	-8.0%	-9.9%
y=6	9.4%	7.5%	5.5%	3.6%	1.6%	-0.3%	-2.3%	-4.3%	-6.2%	-8.2%	-10.1%
y=8	9.0%	7.1%	5.2%	3.3%	1.3%	-0.6%	-2.6%	-4.5%	-6.5%	-8.4%	-10.3%
y=10	8.6%	6.8%	4.8%	2.9%	1.0%	-1.0%	-2.9%	-4.8%	-6.8%	-8.7%	-10.6%

Table A 5. Percentage differences for fluence-weighted angles, fluence to $h_p(10,a)$ conversion coefficients, and fluences, for distance d = 150 and tilt angle a = 30° for positions with a range of (x,y) coordinates, on a rectangular plane above a circular source of radius 15.

Fluence-weighted average angles, ϕ_{fwa} (degrees)											
	x=-10	x=-8	x=-6	x=-4	x=-2	x=0	x=2	x=4	x=6	x=8	x=10
y=0	26.76	27.45	28.13	28.81	29.47	30.12	30.77	31.41	32.04	32.66	33.28
y=2	26.77	27.46	28.14	28.84	29.48	30.13	30.78	31.42	32.05	32.67	33.28
y=4	26.80	27.49	28.17	28.89	29.50	30.16	30.80	31.44	32.07	32.69	33.31
y=6	26.86	27.54	28.22	28.95	29.55	30.20	30.85	31.48	32.11	32.73	33.34
y=8	26.93	27.61	28.29	29.03	29.61	30.26	30.90	31.54	32.16	32.78	33.39
y=10	27.02	27.70	28.37	29.69	29.69	30.34	30.98	31.61	32.23	32.85	33.45

$h_p(10,\alpha)$, difference to value for angle of incidence = 30°											
	x=-10	x=-8	x=-6	x=-4	x=-2	x=0	x=2	x=4	x=6	x=8	x=10
y=0	4.5%	3.6%	2.6%	1.7%	0.8%	-0.2%	-1.1%	-2.1%	-3.1%	-4.1%	-5.0%
y=2	4.5%	3.5%	2.6%	1.7%	0.8%	-0.2%	-1.2%	-2.1%	-3.1%	-4.1%	-5.1%
y=4	4.4%	3.5%	2.6%	1.6%	0.7%	-0.2%	-1.2%	-2.2%	-3.1%	-4.1%	-5.1%
y=6	4.3%	3.4%	2.5%	1.5%	0.7%	-0.3%	-1.3%	-2.2%	-3.2%	-4.2%	-5.2%
y=8	4.3%	3.3%	2.4%	1.4%	0.6%	-0.4%	-1.3%	-2.3%	-3.3%	-4.3%	-5.2%
y=10	4.1%	3.2%	2.3%	0.5%	0.5%	-0.5%	-1.4%	-2.4%	-3.4%	-4.4%	-5.3%

Fluence, difference to value at (x = 0, y = 0)											
	x=-10	x=-8	x=-6	x=-4	x=-2	x=0	x=2	x=4	x=6	x=8	x=10
y=0	6.6%	5.3%	4.0%	2.7%	1.3%	0.0%	-1.3%	-2.7%	-4.0%	-5.3%	-6.6%
y=2	6.6%	5.3%	4.0%	2.6%	1.3%	0.0%	-1.3%	-2.7%	-4.0%	-5.3%	-6.6%
y=4	6.5%	5.2%	3.9%	2.6%	1.3%	-0.1%	-1.4%	-2.7%	-4.0%	-5.4%	-6.7%
y=6	6.4%	5.1%	3.8%	2.5%	1.2%	-0.2%	-1.5%	-2.8%	-4.1%	-5.4%	-6.7%
y=8	6.3%	5.0%	3.7%	2.4%	1.0%	-0.3%	-1.6%	-2.9%	-4.2%	-5.5%	-6.8%
y=10	6.1%	4.8%	3.5%	2.2%	0.9%	-0.4%	-1.8%	-3.1%	-4.4%	-5.7%	-7.0%

Table A 6. Percentage differences for fluence-weighted angles, fluence to $h_p(10,\alpha)$ conversion coefficients, and fluences, for distance d = 200 and tilt angle α = 30° for positions with a range of (x,y) coordinates, on a rectangular plane above a circular source of radius 15.

Fluence-weighted average angles, ϕ_{fwa} (degrees)											
	x=-10	x=-8	x=-6	x=-4	x=-2	x=0	x=2	x=4	x=6	x=8	x=10
y=0	27.55	28.06	28.57	29.08	29.58	30.07	30.56	31.04	31.52	32.00	32.47
y=2	27.56	28.07	28.58	29.10	29.58	30.07	30.56	31.05	31.53	32.00	32.47
y=4	27.57	28.09	28.59	29.12	29.60	30.09	30.58	31.06	31.54	32.02	32.49
y=6	27.60	28.11	28.62	29.16	29.62	30.11	30.60	31.09	31.56	32.04	32.51
y=8	27.64	28.15	28.66	29.21	29.66	30.15	30.64	31.12	31.60	32.07	32.54
y=10	27.69	28.20	28.71	29.70	29.70	30.19	30.68	31.16	31.64	32.11	32.58

$h_p(10,\alpha)$, difference to value for angle of incidence = 30°											
	x=-10	x=-8	x=-6	x=-4	x=-2	x=0	x=2	x=4	x=6	x=8	x=10
y=0	3.4%	2.7%	2.0%	1.3%	0.6%	-0.1%	-0.8%	-1.6%	-2.3%	-3.0%	-3.8%
y=2	3.4%	2.7%	2.0%	1.3%	0.6%	-0.1%	-0.8%	-1.6%	-2.3%	-3.0%	-3.8%
y=4	3.4%	2.7%	2.0%	1.3%	0.6%	-0.1%	-0.9%	-1.6%	-2.3%	-3.0%	-3.8%
y=6	3.4%	2.7%	2.0%	1.2%	0.6%	-0.2%	-0.9%	-1.6%	-2.3%	-3.1%	-3.8%
y=8	3.3%	2.6%	1.9%	1.1%	0.5%	-0.2%	-0.9%	-1.7%	-2.4%	-3.1%	-3.9%
y=10	3.2%	2.5%	1.8%	0.4%	0.4%	-0.3%	-1.0%	-1.7%	-2.5%	-3.2%	-3.9%

Fluence, difference to value at (x = 0, y = 0)											
	x=-10	x=-8	x=-6	x=-4	x=-2	x=0	x=2	x=4	x=6	x=8	x=10
y=0	5.0%	4.0%	3.0%	2.0%	1.0%	0.0%	-1.0%	-2.0%	-3.0%	-4.0%	-5.0%
y=2	5.0%	4.0%	3.0%	2.0%	1.0%	0.0%	-1.0%	-2.0%	-3.0%	-4.0%	-5.0%
y=4	4.9%	3.9%	2.9%	2.0%	1.0%	0.0%	-1.0%	-2.0%	-3.0%	-4.0%	-5.0%
y=6	4.9%	3.9%	2.9%	1.9%	0.9%	-0.1%	-1.1%	-2.1%	-3.1%	-4.1%	-5.1%
y=8	4.8%	3.8%	2.8%	1.8%	0.8%	-0.2%	-1.2%	-2.1%	-3.1%	-4.1%	-5.1%
y=10	4.7%	3.7%	2.7%	1.7%	0.7%	-0.2%	-1.2%	-2.2%	-3.2%	-4.2%	-5.2%

Table A 7. Percentage differences for fluence-weighted angles, fluence to $h_p(10,\alpha)$ conversion coefficients, and fluences, for distance d = 100 and tilt angle α = 60° for positions with a range of (x,y) coordinates, on a rectangular plane above a circular source of radius 15.

Fluence-weighted average angles, ϕ_{fwa} (degrees)											
	x=-10	x=-8	x=-6	x=-4	x=-2	x=0	x=2	x=4	x=6	x=8	x=10
y=0	57.05	57.70	58.33	58.94	59.52	60.09	60.64	61.17	61.69	62.19	62.67
y=2	57.06	57.71	58.34	58.97	59.53	60.10	60.65	61.18	61.69	62.19	62.67
y=4	57.09	57.73	58.36	59.00	59.55	60.12	60.66	61.20	61.71	62.21	62.69
y=6	57.13	57.77	58.40	59.05	59.58	60.15	60.69	61.22	61.74	62.23	62.71
y=8	57.19	57.83	58.45	59.11	59.63	60.19	60.74	61.26	61.77	62.27	62.74
y=10	57.26	57.90	58.52	59.69	59.69	60.25	60.79	61.31	61.82	62.31	62.79

$h_p(10,\alpha)$, difference to value for angle of incidence = 60°											
	x=-10	x=-8	x=-6	x=-4	x=-2	x=0	x=2	x=4	x=6	x=8	x=10
y=0	12.0%	9.3%	6.8%	4.3%	1.9%	-0.4%	-2.6%	-4.7%	-6.8%	-8.7%	-10.6%
y=2	12.0%	9.3%	6.7%	4.2%	1.9%	-0.4%	-2.6%	-4.7%	-6.8%	-8.8%	-10.7%
y=4	11.9%	9.2%	6.6%	4.0%	1.8%	-0.5%	-2.7%	-4.8%	-6.8%	-8.8%	-10.7%
y=6	11.7%	9.0%	6.5%	3.8%	1.7%	-0.6%	-2.8%	-4.9%	-6.9%	-8.9%	-10.8%
y=8	11.4%	8.8%	6.3%	3.6%	1.5%	-0.8%	-3.0%	-5.1%	-7.1%	-9.1%	-10.9%
y=10	11.1%	8.5%	6.0%	1.3%	1.3%	-1.0%	-3.2%	-5.3%	-7.3%	-9.2%	-11.1%

Fluence, difference to value at (x = 0, y = 0)											
	x=-10	x=-8	x=-6	x=-4	x=-2	x=0	x=2	x=4	x=6	x=8	x=10
y=0	19.3%	15.0%	11.0%	7.2%	3.5%	0.0%	-3.3%	-6.6%	-9.6%	-12.5%	-15.3%
y=2	19.2%	15.0%	11.0%	7.1%	3.5%	0.0%	-3.4%	-6.6%	-9.6%	-12.6%	-15.4%
y=4	19.0%	14.8%	10.8%	7.0%	3.3%	-0.2%	-3.5%	-6.7%	-9.7%	-12.7%	-15.4%
y=6	18.8%	14.6%	10.6%	6.8%	3.1%	-0.3%	-3.7%	-6.9%	-9.9%	-12.8%	-15.6%
y=8	18.4%	14.2%	10.3%	6.5%	2.8%	-0.6%	-3.9%	-7.1%	-10.1%	-13.0%	-15.8%
y=10	17.9%	13.8%	9.8%	6.1%	2.5%	-1.0%	-4.2%	-7.4%	-10.4%	-13.3%	-16.0%

Table A 8. Percentage differences for fluence-weighted angles, fluence to $h_p(10,\alpha)$ conversion coefficients, and fluences, for distance d = 150 and tilt angle α = 60° for positions with a range of (x,y) coordinates, on a rectangular plane above a circular source of radius 15.

Fluence-weighted average angles, ϕ_{fwa} (degrees)											
	x=-10	x=-8	x=-6	x=-4	x=-2	x=0	x=2	x=4	x=6	x=8	x=10
y=0	58.04	58.46	58.87	59.27	59.66	60.04	60.41	60.78	61.14	61.49	61.83
y=2	58.04	58.46	58.87	59.28	59.66	60.04	60.42	60.78	61.14	61.49	61.83
y=4	58.05	58.47	58.88	59.30	59.67	60.05	60.43	60.79	61.15	61.50	61.84
y=6	58.07	58.49	58.90	59.32	59.69	60.07	60.44	60.80	61.16	61.51	61.85
y=8	58.10	58.51	58.92	59.35	59.71	60.09	60.46	60.82	61.18	61.53	61.87
y=10	58.13	58.54	58.95	59.73	59.73	60.11	60.48	60.85	61.20	61.55	61.89

$h_p(10,\alpha)$, difference to value for angle of incidence = 60°											
	x=-10	x=-8	x=-6	x=-4	x=-2	x=0	x=2	x=4	x=6	x=8	x=10
y=0	7.9%	6.2%	4.6%	2.9%	1.4%	-0.2%	-1.7%	-3.1%	-4.6%	-6.0%	-7.3%
y=2	7.9%	6.2%	4.6%	2.9%	1.4%	-0.2%	-1.7%	-3.1%	-4.6%	-6.0%	-7.3%
y=4	7.9%	6.2%	4.5%	2.8%	1.3%	-0.2%	-1.7%	-3.2%	-4.6%	-6.0%	-7.3%
y=6	7.8%	6.1%	4.5%	2.8%	1.3%	-0.3%	-1.8%	-3.2%	-4.6%	-6.0%	-7.4%
y=8	7.7%	6.0%	4.4%	2.6%	1.2%	-0.4%	-1.8%	-3.3%	-4.7%	-6.1%	-7.5%
y=10	7.6%	5.9%	4.2%	1.1%	1.1%	-0.5%	-1.9%	-3.4%	-4.8%	-6.2%	-7.5%

Fluence, difference to value at (x = 0, y = 0)											
	x=-10	x=-8	x=-6	x=-4	x=-2	x=0	x=2	x=4	x=6	x=8	x=10
y=0	12.4%	9.8%	7.2%	4.7%	2.3%	0.0%	-2.3%	-4.5%	-6.6%	-8.7%	-10.7%
y=2	12.4%	9.8%	7.2%	4.7%	2.3%	0.0%	-2.3%	-4.5%	-6.6%	-8.7%	-10.7%
y=4	12.3%	9.7%	7.1%	4.7%	2.3%	-0.1%	-2.3%	-4.5%	-6.7%	-8.7%	-10.7%
y=6	12.2%	9.6%	7.0%	4.6%	2.2%	-0.2%	-2.4%	-4.6%	-6.7%	-8.8%	-10.8%
y=8	12.1%	9.4%	6.9%	4.4%	2.0%	-0.3%	-2.5%	-4.7%	-6.8%	-8.9%	-10.9%
y=10	11.9%	9.3%	6.7%	4.3%	1.9%	-0.4%	-2.7%	-4.9%	-7.0%	-9.0%	-11.0%

Table A 9. Percentage differences for fluence weighted angles, fluence to $h_p(10,\alpha)$ conversion coefficients, and fluences, for distance d = 200 and tilt angle α = 60° for positions with a range of (x,y) coordinates, on a rectangular plane above a circular source of radius 15.

Fluence weighted average angles, ϕ_{fwa} (degrees)											
	x=-10	x=-8	x=-6	x=-4	x=-2	x=0	x=2	x=4	x=6	x=8	x=10
y=0	58.54	58.84	59.15	59.45	59.74	60.02	60.31	60.58	60.86	61.12	61.39
y=2	58.54	58.85	59.15	59.45	59.74	60.02	60.31	60.58	60.86	61.13	61.39
y=4	58.54	58.85	59.15	59.46	59.74	60.03	60.31	60.59	60.86	61.13	61.39
y=6	58.55	58.86	59.16	59.47	59.75	60.04	60.32	60.60	60.87	61.14	61.40
y=8	58.57	58.87	59.18	59.49	59.76	60.05	60.33	60.61	60.88	61.15	61.41
y=10	58.58	58.89	59.19	59.78	59.78	60.06	60.35	60.62	60.89	61.16	61.42

$h_p(10,\alpha)$, difference to value for angle of incidence = 60°											
	x=-10	x=-8	x=-6	x=-4	x=-2	x=0	x=2	x=4	x=6	x=8	x=10
y=0	5.9%	4.7%	3.4%	2.2%	1.1%	-0.1%	-1.2%	-2.3%	-3.4%	-4.5%	-5.6%
y=2	5.9%	4.7%	3.4%	2.2%	1.1%	-0.1%	-1.2%	-2.3%	-3.4%	-4.5%	-5.6%
y=4	5.9%	4.6%	3.4%	2.2%	1.0%	-0.1%	-1.3%	-2.4%	-3.5%	-4.5%	-5.6%
y=6	5.9%	4.6%	3.4%	2.1%	1.0%	-0.2%	-1.3%	-2.4%	-3.5%	-4.6%	-5.6%
y=8	5.8%	4.6%	3.3%	2.1%	1.0%	-0.2%	-1.3%	-2.4%	-3.5%	-4.6%	-5.6%
y=10	5.7%	4.5%	3.3%	0.9%	0.9%	-0.3%	-1.4%	-2.5%	-3.6%	-4.7%	-5.7%

Fluence, difference to value at (x = 0, y = 0)											
	x=-10	x=-8	x=-6	x=-4	x=-2	x=0	x=2	x=4	x=6	x=8	x=10
y=0	9.2%	7.2%	5.4%	3.5%	1.7%	0.0%	-1.7%	-3.4%	-5.0%	-6.6%	-8.2%
y=2	9.1%	7.2%	5.4%	3.5%	1.7%	0.0%	-1.7%	-3.4%	-5.0%	-6.6%	-8.2%
y=4	9.1%	7.2%	5.3%	3.5%	1.7%	0.0%	-1.7%	-3.4%	-5.0%	-6.6%	-8.2%
y=6	9.0%	7.1%	5.3%	3.4%	1.7%	-0.1%	-1.8%	-3.5%	-5.1%	-6.7%	-8.2%
y=8	9.0%	7.1%	5.2%	3.4%	1.6%	-0.2%	-1.9%	-3.5%	-5.2%	-6.7%	-8.3%
y=10	8.9%	7.0%	5.1%	3.3%	1.5%	-0.2%	-1.9%	-3.6%	-5.2%	-6.8%	-8.4%